LABORATORI NAZIONALI DI FRASCATI
SIS-Pubblicazioni

LNF-99/031 (IR)
26 Ottobre 1999

A feasibility study of an asymmetric e^+e^- linac-ring collider at $\sqrt{s} \approx 2\,GeV$ with some existing storage rings

Piero Patteri
INFN, Laboratori Nazionali di Frascati, P.O. Box 13, I-00044 Frascati, Italy

Abstract

The feasibility studies and luminosity estimates of some conceivable asymmetric e^+e^- linac-ring colliders are presented. The peculiar features of some storage rings (PETRA, CESR, SPS, PEP II) are discussed in order to achieve a goal luminosity $\mathcal{L} \approx 10^{30} \div 10^{31} cm^{-2} s^{-1}$ at $\sqrt{s} \approx 2\,GeV$. The performances to be provided by a suitable linac, both a superconducting or, when possible, a conventional one, are presented.

Some points which are of concern in the design of the detector, due to the boosting of the outgoing particles in the laboratory frame, are introduced too.

PACS:41.75.L, 13.40.G

Contents

List of Figures

List of Tables

Introduction

A linac -ring collider has been considered in many studies as a machine suitable of providing very high luminosity for a factory of Φ [1,2], J/ψ or B mesons [3,4]. None of these studies grew up to the thorough examination of a Conceptual Design Report. The design goals of such machines were very ambitious, aiming at luminosity $\mathcal{L} \approx 10^{33} \div 10^{34} cm^{-2} s^{-1}$.

These studies identified a few critical points in the project of a linac ring collider, e.g. linac beam power, low ring emittance, peculiar beam beam perturbation, which would have made the realization of such a machine a very challenging task. On the other hand experimental operational knowledge was completely missing, because no machine of this kind has ever been operated. Moreover, all these studies assumed that a high quality and high current electron beam were feasible. The only machine which could have satisfied those requirements was a linac with a superconducting accelerating structure; at that time only a limited experience with that kind of machines was available and it was still to prove they had the reliability and ruggedness required in a factory.

All this probably pushed the projects of the present generation of high luminosity colliders to conservatively exploit at the best the traditional configuration of one or two intersecting storage rings instead of exploring new ways.

In the meanwhile the technology of rf superconducting linac has got impressive achievements, both in the basic performance parameters both in the operational reliability as it is proved by the realization of the TESLA Test Facility at DESY and the activity at the Jefferson Lab. A future proposal of a very high luminosity linac-ring collider will be based on a reliable know how on the main components of the machine. A pioneering small scale experiment would be an valuable contribution to such development providing a test bench of the critical point of beam dynamics.

This note summarizes the feasibility studies carried on in order to propose an asymmetric linac ring collider at $\sqrt{s} \approx 2 GeV$ to measure the nucleon time-like form factors and the multihadronic e^+e^-annihilation cross section. The FENICE experiment at ADONE [5] found unexpected results in this energy range. Although the detector design was optimized for $n\bar{n}$ detection the integrated luminosity was not higher than previous collected in the world and a new experiment is called for. Since the required luminosity is $\mathcal{L} \geq 10^{30}\, cm^{-2} s^{-1}$ some of the most relevant difficulties of a very high luminosity collider are smoothed; nevertheless these studies provided a deeper insight of the problem in accelerator physics and detector design arising in this new configuration. Moreover,

a collider satisfying the requirements for an upgraded FENICE experiment proved to be more flexible than expected andusable in an energy range larger than originally supposed. A brief account of this is given in the sect. 1.3.

A new experiment to measure $e^+e^- \rightarrow n\bar{n}$ with some boosting of the center of mass frame with respect to the laboratory would gain in the detection efficiency of the neutrons near the production threshold. According to the FENICE experience, this is the most desirable feature, together with a higher luminosity, of a new experiment.

The most effective way to provide both luminosity and boosting is colliding an intense positron beam, stored in a high energy ring at $3\,GeV < E_p < 20\,GeV$ against a less intense disposable electron beam of energy $50\,MeV > E_e > 300\,MeV$. The planned activity in the future high energy physics large experiments, and of course economical consideration did not allow to think about a dedicated new machine, pushing to take some existing storage rings (PETRA, CESR, SPS) as candidate for this collider. These preliminary analyses mainly aimed at estimating the luminosity which could be achieved exploiting at the best the performances of the ring with a suitable new or existing linac. Very few ring upgrading, or none at all, were considered but of course a new dedicated interaction section optimized for the peculiar kinematics. Less constraints were assumed in the linac specifications because it is a smaller machine suitable of upgrading in modular way, and it is very versatile for reusing in following activities. Moreover, in the case of the use of an existing injector, any linac upgrading is immediately beneficial to the downstream machine.These analyses are reported in section 3.

A further configuration, which could exploit the Low Energy Ring of PEP II is presented in section 4; it would be the most interesting both for the high luminosity achievable in the present LER setting, i.e. in parasitic mode, both for the wider range of research items, at higher luminosity, which could be addressed if some time for dedicated operation can be allotted in the future.

1 The scientific case

The $e^+e^- \rightarrow hadrons$ annihilation reactions at $\sqrt{s}$ below $2.4\,GeV$ have been studied by the first generation of storage ring ACO , VEPP II , ADONE and later by DCI at luminosity never exceeding $\approx 10^{30}\,cm^{-2}s^{-1}$ and generally much lower.

An estimate of the integrated luminosity collected by the most recent apparata has been attempted. The results are shown in table 1.

Energy	Detector			$\sum \int \mathcal{L}dt$
GeV	DM1	DM2	FENICE	$[nbarn^{-1}]$
$1.6 \div 1.8$	691	432	-	1123
$1.8 \div 2.0$	238	332	144	714
$2.0 \div 2.2$	264	379	194	837
$2.2 \div 2.5$	-	218	57	275

Table 1: Integrated luminosity collected in the mass range $1.6 \geq \sqrt{s}[GeV] \geq 2.5$.

1.1 The FENICE experiment

In 1984 the FENICE experiment on ADONE was proposed in order to measure the neutron electromagnetic form factor and investigate some still open puzzles in the energy range $1.8 < GeV < 3.1$ [6]. The apparatus had no magnetic field so it could not resolve the intricacy of multihadron production but was optimized for neutron and low energy gamma detection [7]. The integrated luminosity for data collection around the baryon threshold was $\approx 350\, nbarn^{-1}$ and collected a sample of $74\, n\bar{n}$ and $76\, p\bar{p}$ pairs [5].

FENICE carried out the first measurement at the threshold of the electric and magnetic form factors of neutron, respectively indicated by G_E and G_M. The results of $G_M^{neutron}$, shown in fig. 1, denies the simple QCD predictions of $G_M^{neutron}/G_M^{proton} = q_d/q_u = -0.5$.

The data on $p\bar{p}$ are in agreement with the previous measurements (see fig. 2b). FENICE could not extend the measured range below $s = 3.7\, GeV^2$ so it was not possible a full measurement of the steep decrease of proton form factor from the boundary between the unphysical and the timelike region, clearly measured at LEAR [8], The peculiar form factor behaviour near $p\bar{p}$ threshold is not fitted by any simple form factor model. On the other hand the FENICE multihadronic production below the $p\bar{p}$ threshold shows a narrow dip, as shown in fig. 2a. Old data of DM2 and more recent preliminary results from the photoproduction experiment E831 [1] are consistent with this picture. If these effects are correlated the behaviour of the proton form factor is consistent with the existence of a narrow resonance below $p\bar{p}$ threshold, as shown in the fits in fig. 2.

[1] Preliminary data presented at the Nucleon 99 Workshop, Frascati, June 1999

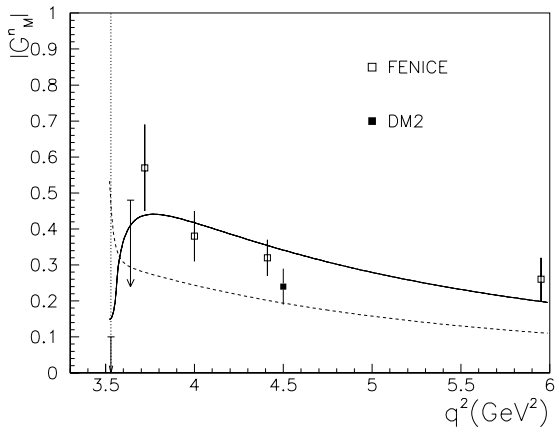

Figure 1: Neutron time-like form factor as measured by the FENICE experiment in the hypothesis $|G_E| = 0$. Dashed line shows the pQCD prediction $G_M^{(n)} = \frac{1}{2}G_M^{(p)}$. The figure is taken from ref. [5]

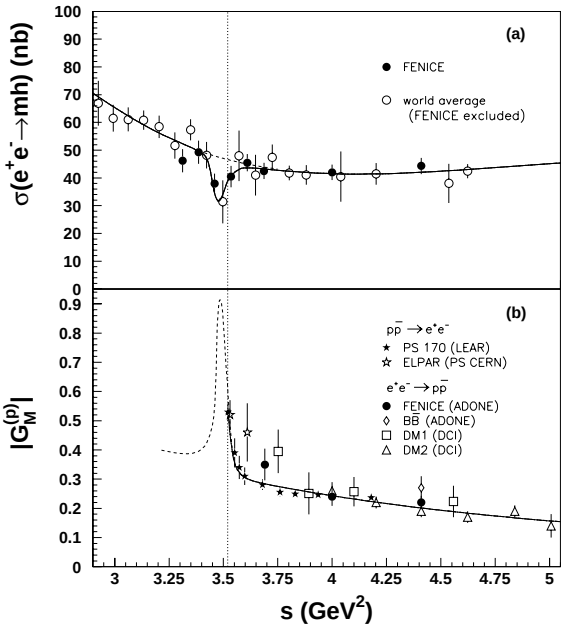

Figure 2: Multihadronic cross-section (upper plot) and proton form factor (lower plot) as a function of the center of mass energy. A combined fit is also shown. The figure is taken from ref. [5]

1.2 The luminosity relationship

The luminosity of an asymmetric linac-ring collider is given by

$$\mathcal{L} = \frac{n_e n_p f_c}{4\pi\sigma_x\sigma_z} = \frac{I_M I_{ring}}{4\pi\sigma_x\sigma_z}\frac{t_M f_M}{e^2 n_b f_{ring}} \tag{1}$$

The meaning of the parameters is given in the footnote [2].

The stored beam size is proportional to $\epsilon^{1/2}$, therefore its energy dependence is

$$\sigma_x = \gamma_p\sqrt{\frac{\epsilon_{np}\beta_x}{1+k}} \tag{2}$$

$$\sigma_z = \gamma_p\sqrt{\frac{\epsilon_{np}\beta_z k}{(1+k)}} \tag{2'}$$

The γ_p factor in eqs. 2, 2' account for the energy dependence of the emittance in a storage ring. The expressions for beam size in eqs. 2, 2' are valid only at a beam waist, where dispersion η and η',β' are assumed vanishing.

The linac beam size can be expressed in a similar form valid in both planes

$$\sigma_i = \sqrt{\epsilon_{ne}\beta_i/\gamma} \qquad (i = x, z) \tag{3}$$

The constraint between γ_e and γ_p at constant c.m. energy

$$\sqrt{s} = 2m_e\sqrt{\gamma_e\gamma_p} \tag{4}$$

coupled with the energy dependence of the emittance of a ring and a linac given in eq. 2 and 3 results in a strong dependency of luminosity on linac energy

$$\mathcal{L} = C_L\frac{\gamma_e^2}{s^2\epsilon_{np}\sqrt{k}\beta_x\beta_z}\frac{n_e n_p f_c}{4\pi} \tag{5}$$

where $C_L \equiv 16m_e^4 = 1.088\cdot 10^{-12}\ GeV^4$

It is worthwhile noting that if an increase of s is accomplished by a corresponding increase of γ_e the luminosity is not affected. These simple relationships indicate that the optimal configuration would have the ring operating at the minimum energy and the highest linac beam energy. However, both the cost of the linac, roughly proportional to γ_e, and the requirement on stability and lifetime of the stored beam, better at higher γ_p,

[2] $n_{e(p)}$ is the number of electrons (positrons) in each bunch; f_c $[Hz]$ is the frequency of collision at the interaction point;I_{ring} $[A]$ is the current in the storage ring, divided in n_b bunches, circulating with orbital frequency f_{ring} $[Hz]$; I_M $[A]$, t_M $[s]$ and f_M $[Hz]$ are respectively current, duration and repetition rate of the linac macropulse; σ_x, σ_z $[cm]$ are respectively the horizontal and vertical size of the beam at the interaction point.

ask for an optimization taking into account more that the simple luminosity dependence on cross section at the interaction point.

A luminosity limit seems to be set , as far as the electron beam is concerned, by the huge power required to accelerate a high average current beam and by radiation safety problems when wasting such power in a beam dump; this would impose a reduction of the duty cycle and therefore of the luminosity.

This problem is the same to be faced at a Free Electron Laser facility for industrial application, where the high average power is a key parameter. The successful test of the beam energy recovery, recentely accomplished at TJNAL, pushed forward the luminosity limit of linac-ring collider , as far as the linac beam power is concerning, by an order of magnitude. This possibility is more extensively presented in section 5.

1.3 The energy range

The invariant mass M_{inv} produced in an asymmetric head-on collision of positron and electron beams respectively with energy E_p and E_e is given according to eq. 4 by

$$M_{inv}^2 = 4E_pE_e \tag{6}$$

The plot of this equation for some relevant values of M_{inv} between the $n\bar{n}$ threshold and the $\tau^+\tau^-$ region is shown in fig. 3. The operational range of the rings is shown by the horizontal bars at the bottom of the figure. The lower limit of the SPS has been set at the energy corresponding to a horizontal damping time $\tau_x \approx 500\,ms$.

Since a repetition of the FENICE experiment aims to accurately measuring the reaction $e^+e^- \rightarrow baryons$ the geometrical acceptance and the detection efficiency of the detector are primary goals. The boosting of the c.m. frame is a relevant parameter of the overall efficiency because it brings about the maximum pair opening, the angular distribution and the particle energy in the laboratory frame. The c.m. frame speed

$$\beta_{CM} = \frac{P_p - P_e}{\sqrt{M_{inv}^2 + (P_p - P_e)^2}} \tag{7}$$

with respect to the laboratory is shown in fig. 4 at the values of some M_{inv}.

1.3.1 Extension to J/ψ and ψ' region

Fig. 3 clearly shows that the mass range of the ψ family can be reached with linac energy 300 MeV at CESR operating at $\approx 8\,GeV$ and even less at PETRA and SPS; if this energy can be reached the baryon production at J/ψ will provide a useful calibration tool.

This option can provide a distinct advantage for some measurements due to the large boosting. It will have additional interest if the c.m. energy spread will be better than a

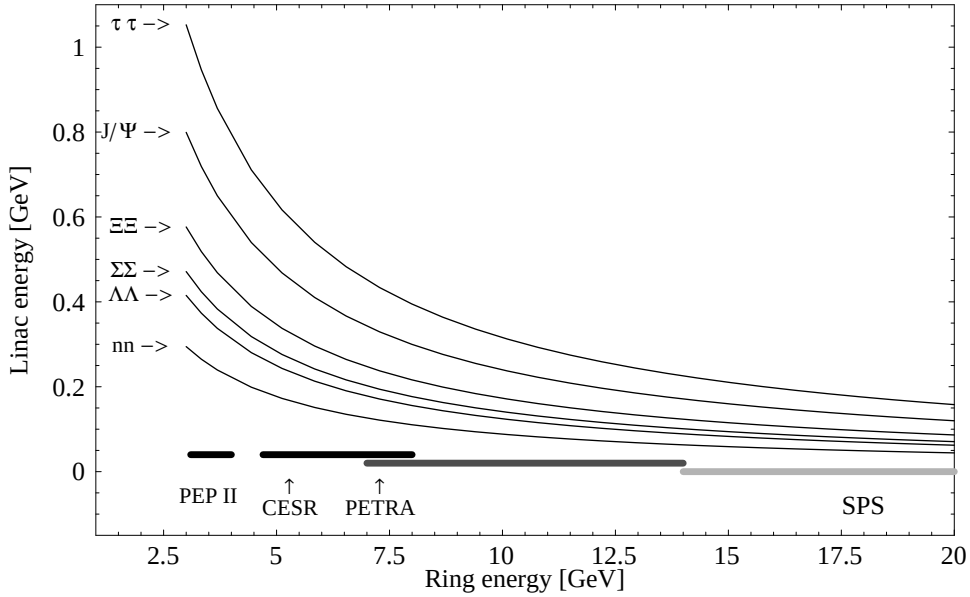

Figure 3: Parametric curves at constant $\sqrt{s}$ corresponding to baryon pair masses, J/ψ and $\tau^+\tau^-$ pair in $E_e \ vs \ E_p$ plane.

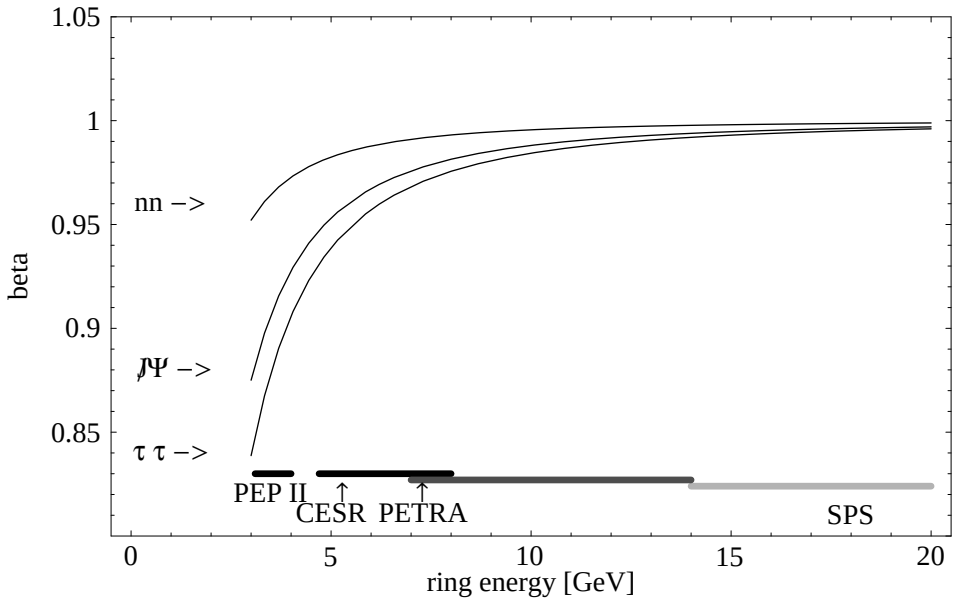

Figure 4: Curves of $\beta_{CM} \ vs \ E_p$ at constant $\sqrt{s}$ corresponding to baryon pair, J/ψ and $\tau^+\tau^-$ pair masses.

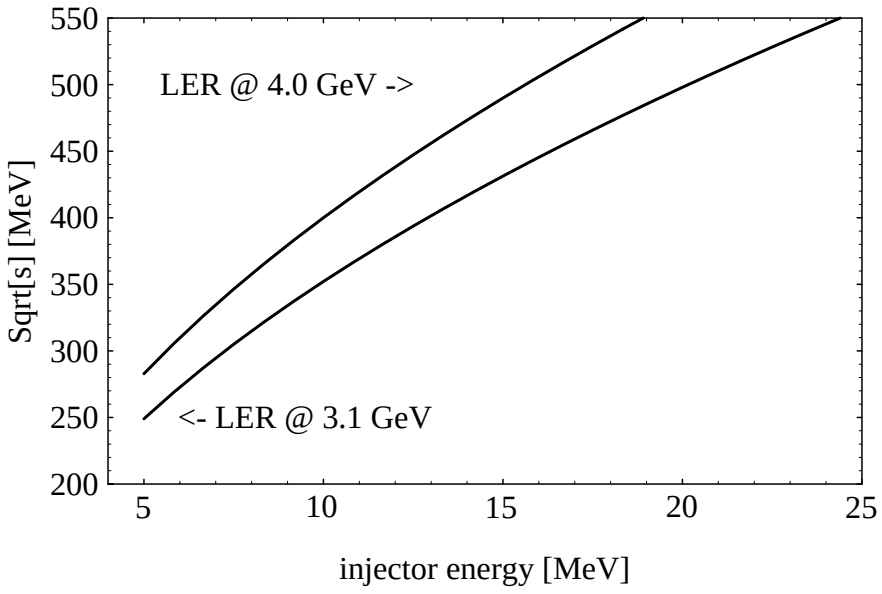

Figure 5: Invariant mass $\sqrt{s}$ attainable at the Low Energy Ring of PEP II as a function of the injector energy.

typical ring collider. Actually, the uncorrelated energy spread in a superconducting linac is $\Delta E/E \approx 10^{-3} \div 10^{-4}$, which is comparable with a typical storage ring parameter $\Delta E/E \geq 5 \cdot 10^{-4}$; since a monochromatization scheme is well suited to a linac-ring collider this possibility deserves further insight as a potential $charm - factory$.

The possibility of extending the useful range of a linac-ring collider increasing the electron beam energy is suggested by the impressive progress in sc cavities achievement, which improved the gradient from $5\,MV/m$ (CEBAF project, 1985) to $25\,MV/m$ (TESLA project, 1996) aiming now to a gradient $> 30\,MV/m$.

1.3.2 A first step at $\pi\pi$ threshold

In the configurations that will be described in the section 3 the possibility of a first intermediate step toward the design energy range was never considered. It is worth noting now that in any case a high quality $\approx 10 \div 20\,MeV$ injector is the first stage of the sc linac. If such a beam collides with the LER ring of PEP II , which is the lowest energy ring considered in this note, it would provide collisions at the threshold of $\pi^+\pi^-$ and $\pi^+\pi^-\pi^0$ production, as shown in fig. 5.

This energy range was only marginally studied at the earliest storage rings. The low statistics of the available data on hadronic production gives the largest contribution to the error in the theoretical calculation of the muonic $g-2$ factor. The possibility of

improving the statistics operating DAΦNE at lower energy has been considered [9], but the availability of machine time and the performances achievable at low energy are not asserted up to now.

The collision of a low energy linac beam with a high energy e^+ beam stored in ADONE was proposed [10] at the beginning of the construction of LISA, a small sc linac operated in the LNF in 1994. The realization of a similar experiment with the injector required for this collider would provide both a contribution to a fundamental measurement and would be a first test bench for any peculiar behaviour of a linac-ring collider.

2 The machine and the experiment entangling at the $n\bar{n}$ threshold region

The analysis presented in this section is based on the kinematical condition which would exist at CESR-linac collider, i.e. a positron energy of $5.3\,GeV$ and an electron beam of $190\,MeV$. Of course substantial changes happen if the energy asymmetry i.e. the β_{CM} velocity is different, as would be in collider realized at PETRA, SPS or PEP II but since the CESR based collider is a midrange configuration among those presented in this note, and it is the only one studied up to now with some details, it is reported here as a review of the peculiar problems of the design of an interaction region at an asymmetric linac-ring collider.

The relativistic trasformation of the trajectory angles from the c.m. frame to the laboratory frame [3] depends on both the c.m. momentum $\mathbf{p}_{cm}$ of the particles both on the relative velocity β_{CM} of the frames.

2.1 The pair angular distribution

The smooth angular distribution $f(\theta_{cm})$ of the pair particles in the c.m. frame is shrinked in the forward direction (positron direction) according to

$$p_{\perp lab} = p_{\perp cm} \qquad = p_{cm}\sin\theta_{cm} \tag{8}$$

$$p_{\|lab} = \gamma_{CM}(p_{\|cm} + \beta_{CM}\frac{\sqrt{s}}{2}) \qquad = \gamma_{CM}(p_{cm}\cos\theta_{cm} + \beta_{CM}\frac{\sqrt{s}}{2}) \tag{9}$$

$$\theta_{lab} = \arctan\frac{p_{\perp lab}}{p_{\|lab}} \qquad = \arctan\frac{p_{cm}sin\theta_{cm}}{\gamma_{CM}(p_{cm}\cos\theta_{cm} + \beta_{CM}\frac{\sqrt{s}}{2})} \tag{10}$$

where $p_{cm} = \sqrt{p^2_{\perp_{cm}} + p^2_{\|_{cm}}}$ and $\sqrt{s}/2$ are respectively the momentum and the energy of each particle in a pair.

[3] The capital indexes identify the c.m. frame kinematical parameters, while the lower case indexes are used to label the particle parameters (momentum, energy...). Bold and plain types respectively indicate vectorial quantities and the related module.

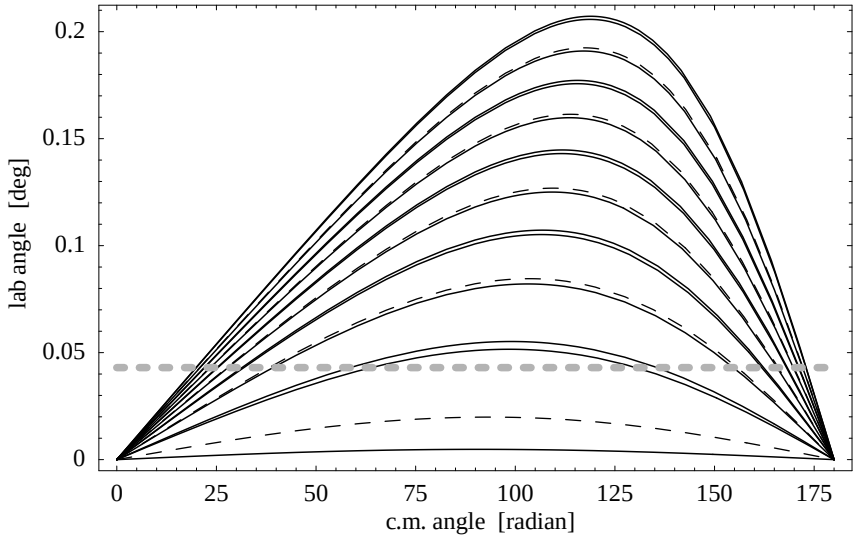

Figure 6: Laboratory exit angle vs. center of mass emission angle for protons (dashed lines) and neutrons (continuous line). The beam energy is $5.3\,GeV$ for positron and $170 \div 220\ MeV$ in $5\ MeV$ steps for electrons.

In section 2.3 it will be shown that to get the required focusing of the optical function at the IP the closest quadrupoles must be placed $\approx 1\,m$ far from the collision point. An analysis of the effect of these quadrupoles on the geometrical acceptance of downstream particles has been carried out in some detail on the basis of the interaction region layout designed for the collider at CESR presented in [11]. An iron core electromagnetic quadrupole type can barely provide the required focusing strength and will intercept a large fraction of the particles, so only permanent magnet or superconducting quadrupoles are suitable for the inner quadrupoles. Since they have different outer radii and inner bulk distributions, they affect in different way the geometrical efficiency.

2.1.1 The pair angular distribution at $n\bar{n}$ threshold

The plot of $\theta_{lab}\,vs\,\theta_{cm}$ for proton and neutrons around the threshold ($1860 < \sqrt{s}\,[MeV] < 2200$) is shown in fig. 6. The horizontal dashed line corresponds to the angular cut caused by a permanent magnet quadrupole of the type used in CESR, starting at $150\,cm$ downstream the IP and cladding the pipe up to an outer radius of $6.4\,cm$.

The angular opening of the baryon trajectories just a few MeV above the threshold is so narrow that a nonegligible fraction goes through the bore or the body of the first downstream quadrupole. This problem is more relevant at higher boosting. The effect on the detection efficiency in this critical region, where the baryon production is heavily

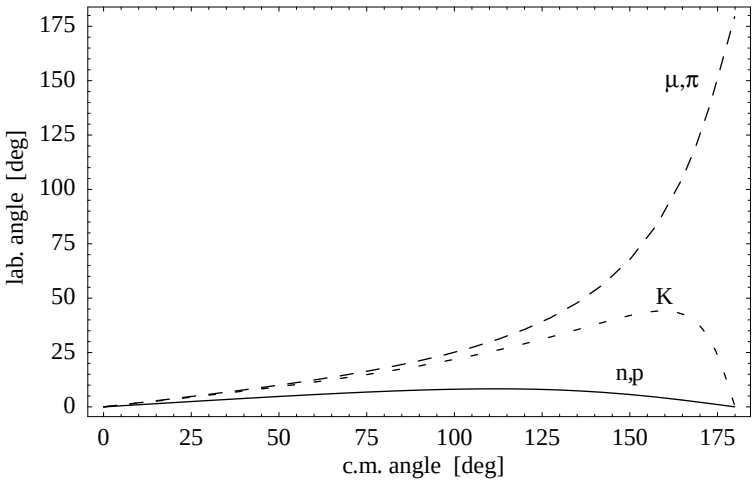

Figure 7: Laboratory exit angle vs. center of mass emission angle for light hadrons and muons. The beam energy is $5.3\,GeV$ for positron and $190\,MeV$ for electrons, corresponding to $s = 4.0\,GeV^2$.

affected by the phase space limitation too, is to be carefully estimated. A device to detect the hadronic shower produced by a baryon interacting in the body of the quadrupole should be envisaged, since it is likely that most of the shower particles pass the small thickness of a permanent magnet or iron-less superconducting quadrupole.

Depending on the machine layout, it is conceivable also to detect neutron going through the pipe and quads and exiting from the first downstream magnet. In this way nearly 100% of the downstrean solid angle would be covered.

The trajectories of $p,\ \bar{p}$ are of course affected by the magnetic elements so the detection efficiency of small angle $p,\ \bar{p}$ needs a deeper study.

The other two-body reactions have a wider angular exit range, so the background in the baryon pair sample due to more frequent collinear events is strongly reduced. The curves in fig. 7 show the laboratory exit angle of π, k and barions as a function of the center of mass emission angle.

Although the boosting is desirable to increase the detection efficiency, increasing the energy available in the interaction of slow output particles, it makes more difficult to distinguish the baryons from other hadrons because the rest mass energy available in the annihilation star of a $\bar{n}$ or $\bar{p}$ is now only a fraction of the total energy involved. However the lighter hadrons can be identified due to wider angular distribution and their peculiar angular correlation.

2.2 Energetic and angular resolution

The energy and angular spread resulting from the collision of two beams in a symmetric ring collider are easily given by the convolution of the initial gaussian distributions. The same it is assumed here for the linac-ring for simplicity, although the distribution of a linac beam is not gaussian, and a proper folding of the distribution would give a better estimate of the tails.

2.2.1 Energy spread

The relative spread of collision energy $\sqrt{s}$ is

$$\frac{\Delta\sqrt{s}}{\sqrt{s}} = \frac{\Delta\sqrt{E_p E_e}}{\sqrt{E_p E_e}} = \frac{1}{2}\sqrt{\left(\frac{\Delta E_e}{E_e}\right)^2 + \left(\frac{\Delta E_p}{E_p}\right)^2} \tag{11}$$

The electron beam relative energy spread $\Delta E_e/E_e$ is mainly given by the absolute energy spread ΔE_e^{inj} at the injector exit. Henceforth up to the final energy E_e the relative energy spread is reduced because all electrons have the same energy gain during the acceleration while the effect of various heating mechanisms weakens as the beam energy increases, so that

$$\frac{\Delta E_e}{E_e} = \frac{\Delta E_e^{inj}}{E_e} \tag{12}$$

On the contrary, the energy spread of the stored beam increases with the energy [4]

$$\frac{\Delta E_p}{E_p} = E_p\sqrt{\frac{C_q}{J_\epsilon \rho}} \tag{13}$$

therefore both terms in eq. 11 increase with the energy ratio $R = E_p/E_e$. Again, as shown in fig. **??** for two typical rings, the operation at the lowest E_p gives the best performances.

2.2.2 Angular spread

The momentum conservation implies

$$\mathbf{p}_\gamma = \mathbf{p}_p + \mathbf{p}_e$$

where $\mathbf{p}_\gamma$ is the momentum of the virtual photon coming from the electron-positron annihilation. The direction of $\mathbf{p}_\gamma$ is the axis of the angular distribution of the decay products,

[4] In eq. 13 $C_q = 1.468 \cdot 10^{-6}\, m/GeV^2$, J_ϵ is the energy damping partition number and ρ is the magnetic bending radius

so its rms value $\sqrt{< x'^2_\gamma >}$ is the intrinsic spread to be convoluted with the nominal angular distributions, e.g. that in fig. 6. Assuming that energy asymmetry is large enough that

$$|\mathbf{p}_{\perp\gamma}| << |\mathbf{p}_{\|\gamma}|$$

then in a generic plane (a=x,z) it is

$$a'_\gamma = a'_e \frac{p_e}{p_\gamma} + a'_p \frac{p_p}{p_\gamma} \tag{14}$$

The rms value $\sigma'_\gamma \equiv \sqrt{< a'^2_\gamma >}$ can be expressed [5]as a function of σ'_e and σ'_p

$$\sigma'_\gamma = \left(\sigma'^2_e \left(\frac{p_e}{p_\gamma}\right)^2 + \sigma'^2_p \left(\frac{p_p}{p_\gamma}\right)^2 \right)^{\frac{1}{2}} \tag{14'}$$

In a ring the rms divergence at a beam waist is given by

$$\sigma'_x = \gamma_p \sqrt{\frac{\epsilon_{np}}{(1+k)\beta_x}} \tag{15}$$

$$\sigma'_z = \gamma_p \sqrt{\frac{\epsilon_{np} k}{(1+k)\beta_z}} \tag{15'}$$

In a linac it is

$$\sigma'_i = \sqrt{\frac{\epsilon_{ne}}{\gamma_e \beta_i}} \qquad (i = x, z) \tag{16}$$

Combining the eqs. 15, 16 and 4 with eq. 14' the rms of distribution of emission axes is expressed as a function of the machine energies and beam parameters

$$\sigma'_{x\gamma} = \left(\frac{\epsilon_{ne}}{\gamma_e \beta_{xe}} \left(\frac{p_e}{p_p - p_e}\right)^2 + \frac{\gamma_p^2 \epsilon_{np}}{(1+k)\beta_{xp}} \left(\frac{p_p}{p_p - p_e}\right)^2 \right)^{\frac{1}{2}} \tag{17}$$

$$\sigma'_{z\gamma} = \left(\frac{\epsilon_{ne}}{\gamma_e \beta_{ze}} \left(\frac{p_e}{p_p - p_e}\right)^2 + \frac{\gamma_p^2 \epsilon_{np} k}{(1+k)\beta_{zp}} \left(\frac{p_p}{p_p - p_e}\right)^2 \right)^{\frac{1}{2}} \tag{17'}$$

The angular spread of the emission axis is to be compared with the angular opening of the pair at $\sqrt{s}$ just above the threshold. Eqs 17 and 17′ can be expressed as a function of the energy ratio $R \equiv E_p/E_e$ and the c.m. energy $\sqrt{s} = 2\sqrt{E_p E_e}$

$$\sigma'_{x\gamma} = \left(\frac{\epsilon_{ne}}{\beta_{xe}} \frac{2m_e}{\sqrt{s}} \frac{\sqrt{R}}{(R-1)^2} + \frac{\epsilon_{np}}{(1+k)\beta_{xp}} \frac{s}{4m_e^2} \frac{R^3}{(R-1)^2} \right)^{\frac{1}{2}} \tag{18}$$

$$\sigma'_{z\gamma} = \left(\frac{\epsilon_{ne}}{\beta_{ze}} \frac{2m_e}{\sqrt{s}} \frac{\sqrt{R}}{(R-1)^2} + \frac{\epsilon_{np} k}{(1+k)\beta_{zp}} \frac{s}{4m_e^2} \frac{R^3}{(R-1)^2} \right)^{\frac{1}{2}} \tag{18'}$$

[5]Indication of a (or explicitly x, y) plane is neglected for simplicity.

A comparison of σ'_x,, $\sigma'_z$and the maximum opening of a $n\bar{n}$ pair obtained assuming the CESR optical parameters [11] is shown in fig. 9.

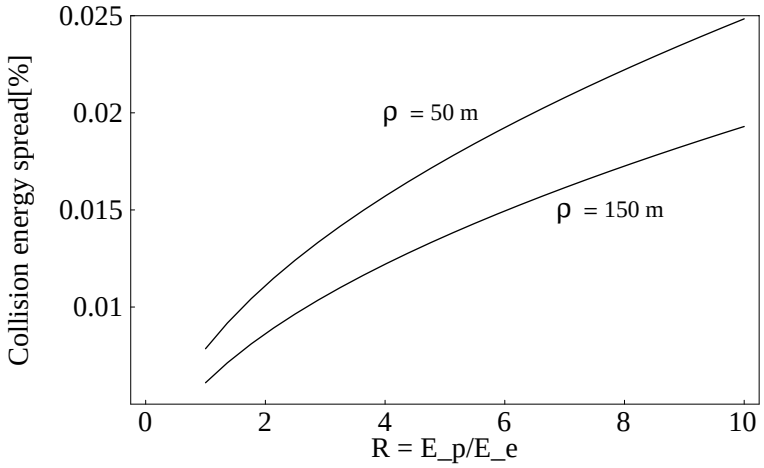

Figure 8: Relative collision energy spread vs $R = E_p/E_e$.

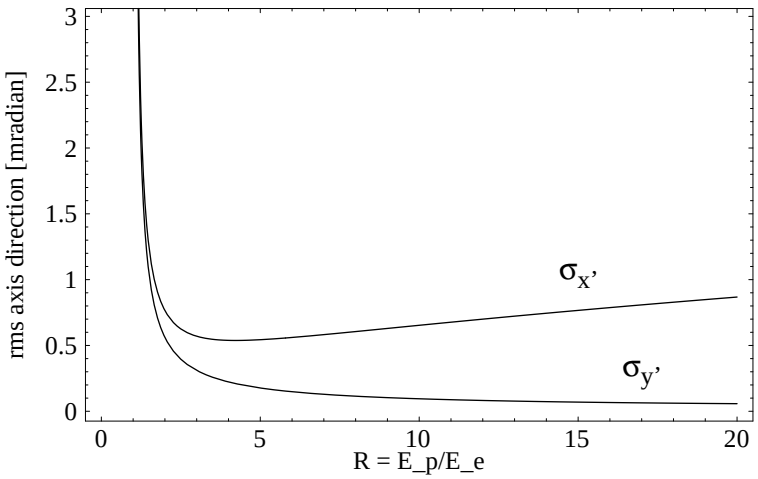

Figure 9: Collision axis angular spread vs $R = E_p/E_e$.

2.3 The interaction region layout

The magnetic lattice of all the rings considered in this note is composed of FODO arcs, joined by straight sections where generally the dispersion is cancelled $\eta = \eta' = 0$. This gives large freedom in the design of the interaction region because only β_x, β_z and their derivatives must be matched at the arc ends, so it can be assumed that the same inner part of the interaction region lattice can be inserted in the straight section of whatsoever ring with some adjustment of focusing strength and spacing of the outer quadrupoles.

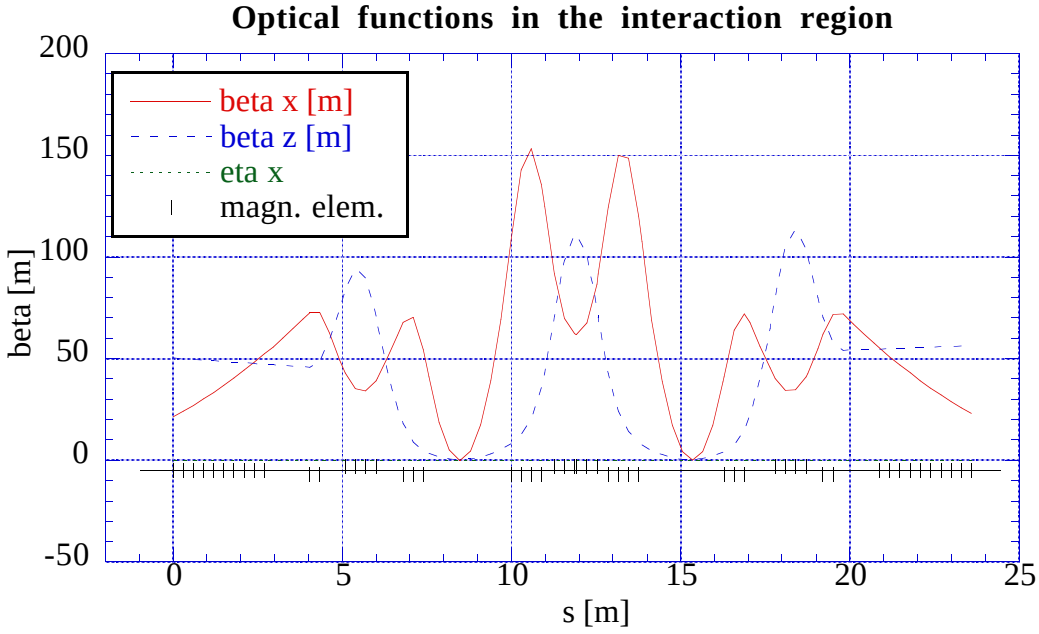

Figure 10: Optical function β_x, β_z of the lattice designed for a collision point in the North Interaction Point at CESR [11].

The interaction region designed for the CESR collider is shown in fig. 10; note that the collision point is moved $\approx 3.5\,m$ aside from the straight section symmetry point in order to have the most of the experimental hall length exploitable for time-of-flight measurements.

A pratical limit to transportability of an IR design to an higher energy ring is given by the maximum quadrupole gradient; the requirements of strong focusing and small interference with outgoing particles restrict the choice to permanent magnet or iron-less superconducting quadrupoles which provide a gradient $\approx 20 Tesla/m$, corresponding to the focusing strength $k \approx 1\,m^{-2}$ @ $5.3\,GeV$ required in the CESR-type interaction region.

2.3.1 Multihadron production

The measurement of the cross sections of and their branching ratio is not the primary goal of FENICE II, but the intriguing correlation between the dip in total hadronic production at 1820 MeV and the steep rise of the proton cross section at threshold, shown in fig.2 urges that the capability of multitrack measurement is not overlooked.

2.3.2 A schematic detector

Following the considerations of the previous sections a block schematic of the part scomposing the detector around the interaction region can be drawn, as shown in fig. 11

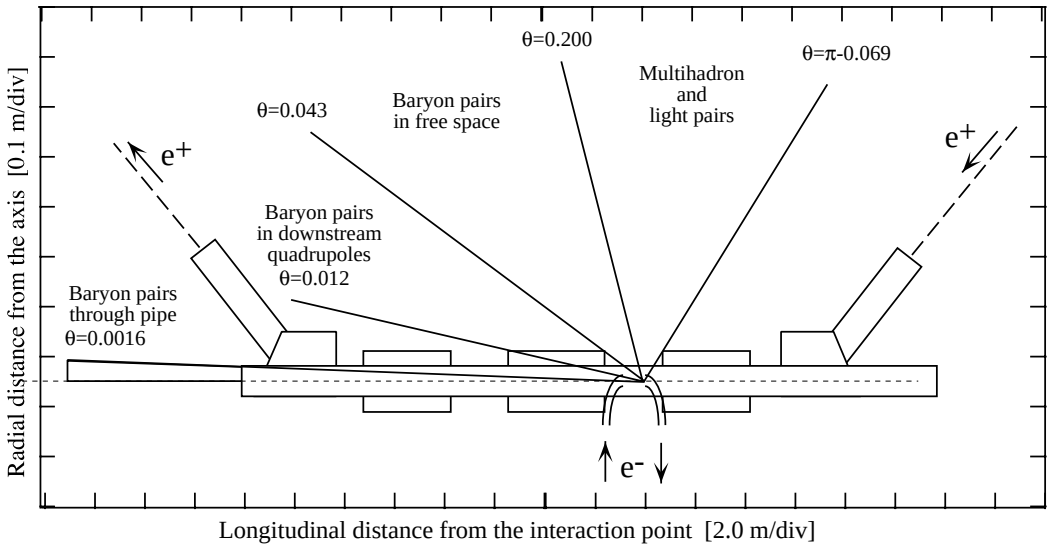

Figure 11: Schematic layout of the detector parts and boundary of the particle angular distributions around the interaction point.

3 The first machine configurations

It has been already pointed out that the most realistic way to realize the first linac-ring collider is to exploit an existing storage ring which is to be filled of positron. This constraint ruled out some rings where a positron source is not available. The availability of some machine time for the experiment in a reasonably near future was another obvious constraint; this ruled out, beyond the positron availability, the large rings fully dedicated to synchrotron radiation users. Since operating energy $\approx 5\,GeV$ and high stored current was also required the possibility was drastically reduced to PETRA, CESR and SPS. A preliminary estimate of the performance achievable at these machines has been carried out starting in October 1996. The notes and papers on these studies refers to different stage of deepening and understanding of the problems, and often with different boundary conditions for their solution, so their results are not directly comparable. Here a chronologically ordered review is presented and a final comparison, as far as possible, is carried out. The performances estimates in different configuration are summarized in table 3.

3.1 TTF-PETRA

A number of features made of PETRA the first choice for this study [12]:

- the ring is now used as injector in HERA and for a limited synchrotron radiation program, so a large amount of machine time should be available.
- the energy range spans from the injection energy of $7\,GeV$ up to $14\,GeV$, requiring only a $150\,MeV$ linac at $n\bar{n}$threshold.
- the TESLA Test Facility hardware and know how could eventually be exploit for the superconducting linac, reducing the capital cost.

The first TTF-PETRA proposal was conceived as a collider exploiting the existing hardware, i.e. PETRA and the TESLA Test Facility (TTF) linac. Since the TTF energy is much higher than required some attention was dedicated to a possible linac optimization to increase the duty cycle trading off the cavity gradient at constant beam power. A major problem arose by the different rf frequency of the ring and linac; however other joined uses of PETRA and TTF which were under study required the solution of this problem, so it was considered not a peculiar problem of the linac ring collider. A serious restriction of the possible performances is the maximum storable current in few bunches $< 100\,mA$, due to the high impedance of the pipe and rf cavities. A large current upgrading was foreseen in some papers presenting a proposal of a $B-factory$ at PETRA, but it required large feedback and rf cavity improvements so it was not taken into account in the luminosity estimate.

The then view of the linac ring collider as a minimal cost and short schedule machine was compatible only with limited additional hardware; moreover the DESY planned activities (HERA luminosity upgrade, TTF and TESLA program) left few time to the accelerator group for the development work required by the linac ring collider. This situation put in stand-by the idea of proposing this collider at DESY. Anyway it is to note that if some new features assumed in the following part of this study, namely a dedicate small sc linac, were applied to PETRA it would possible to achieve excellent performances well above the goal of $\mathcal{L} = 10^{30}\, cm^{-2} s^{-1}$ at a minimal cost, due to the concentration of know how and hardware existing at DESY.

3.2 CESR

The storage ring CESR at the Wilson Lab of the Cornell University was taken into account because it routinely stores current higher than $100\, mA$; it has been operating as a $B - factory$ since 1979 with a number of upgrading keeping the world luminosity record. Short term development program should raise the current to $500\, mA$. The laboratory is actively pursuing the approval of a new ring, to be placed side by side to the existing one, to remain in the forehead of $B - factory$ physics, so there were hope that CESR could be available for some time; moreover a new, or renewed linac, required for the $n\bar{n} - factory$, would become later part of the upgraded injection system for the new machine.

3.2.1 CESR and a sc linac

The first luminosity estimate simply changed the machine parameters from PETRA to CESR, with some more freedom in the specification of the electron accelerator. Again it was considered a small sc linac based on the TTF know how [13,14], and later also a CW race track microtron [15]. The crucial point for the latter option is that the expected luminosity from CESR at $500\, mA$ in 45 bunches is $10^{33} cm^{-2} s^{-1}$; therefore the required luminosity could be obtained with a CW $500\, \mu A$ beam, or even less if the same ring current can be accumulated in a smaller n_b (see eq. 1) However, the construction of a new injector did not fit the short term program of the laboratory, so it was decided to explore if the goal luminosity could be reached using at the best the existing injection system with some upgrading.

3.2.2 CESR and the existing injector

The configuration using CESR and its existing injector has been that more extensively studied among those presented in this note. The analysis of the geometrical efficiency of an hypothetical detector in section 2 have been based on the design described in the note [11] which summarizes the results of a stage at the Wilson Laboratory.

The average current from the $60\,Hz$ CESR injector is $\approx 10\,\mu A$, which would provide a luminosity of $4 \cdot 10^{28}$ only. A glance at the luminosity equations 1 shows that the luminosity is given by two classes of factors: 'current' factors, i.e. n_e,n_p,f_c, I_M,$n_b \ldots$, and 'lattice' factors, i.e. σ_x, σ_z, ϵ, $k \ldots$ Of course they cannot be adjusted in arbitrary way because they affect the beam behavior elsewhere, but the first attempt is to push each of them to the best, later looking for the possible trade off.

The $150\,nC$ charge of each macropulse can be distributed with different patterns within the $2.56\,\mu s$ duration which is the same of one turn revolution of the stored beam; the best for our purpose is a train of 15 pulses of $10\,nC$ or possibly 9 pulses of $15\,nC$. Since the single bunch current limit in CESR is higher than $50\,mA$, an improvement of a factor 3 or 5 can be obtained respectively reducing n_b to 15 or 9.

The remaining improvement must be given by the 'lattice' factors. It was assumed that the available experimental hall were the North Hall, once used by the CUBS experiment. This required some new lattice design around that North Interaction Point (NIP), because in last years any effort aimed at increasing the luminosity at the South Interaction Point, where is the experiment CLEO, without any constraint to keep usable the NIP. The layout of the new NIP was designed taking apart as far as possible the last focusing quadrupoles in order to provide the room required to bring, to squeeze and extract the linac beam at the IP and to have the widest angular acceptance of the baryon pairs at threshold (see section 2.1.1). The new optics at the IP provided a beam section of near round shape suitable to matching the linac beam; the section can be much smaller than that of the CLEO interaction point if low emittance operation is assumed.

CESR has been sometime operated as a dedicated synchrotron radiation source with a low emittance lattice. Other lattice modification, increasing the damping partition number J_x up to 2, had been experimented too. All this justified the design of the collider with a ring emittance near the theoretical minimum achievable with the FODO lattice of CESR. All these factors together gave a luminosity of $\approx 2 \cdot 10^{30}\,cm^{-2}s^{-1}$, but some assumptions on the beam quality and stability, namely of the linac beam, needed further insight to be asserted. The $10\,nC$ pulses provided by the existing gun have an intolerably high emittance, so a new gun is mandatory. The state of art of rf gun for the most challenging FEL experiments have the required level of performances providing normalized emittance $\epsilon_n \approx 10^{-5}\,m$, but usually are followed by a modern linac optimized to reduce the effect of the wakefields. The possibility of accelerating $10\,nC$ bunches in a SLAC type S-band linac without a dramatic emittance worsening is a challenging task. Improvements of the energy spread and stability had to be achieved too.

The tune shift ξ induced by the beam beam perturbation at IP would be intolerably high if compared to common achievements in storage ring. However, the stored beam would collide with the linac beam at $60\,Hz$, and the time between each collision is comparable with the damping time, so it is doubtfull that a resonance effect could drive particles

to large amplitude oscillations affecting the lifetime. Anyway this point deserved further study and simulations because the collision configuration is very different from the standard one used in code simulation.

In conclusion the thorough examination of the possible performance at CESR indicate that the improvements of both the 'current' and 'lattice' factors can be achieved as far as the ring is concerned. The linac 'current' factors can be achieved too, but it appears very hard to do at the same time the 'lattice' factors. Although the feasibility of a linac ring collider using a room temperature linac, and namely the CESR injector linac, cannot be rejected at this stage, it is clear that the cost - performance ratio favours a configuration using a superconducting linac.

3.3 SPS

The feasibility of a linac ring collider using the SPS at CERN was the last considered in this first group of machines. The SPS operated as a proton-antiproton storage ring for SP$\bar{\text{P}}$S collider, and is currently used as positron injector for LEP. Its energy range for positron acceleration is wider than PETRA, extending from 3.5 up to 20 GeV, but the range usable for storing positron is smaller, as mentioned in section 1.3, due to lifetime and instability at lower energy. In this note a positron energy of $14\,GeV$ is assumed corresponding to an horizontal damping time $\tau_x \approx 140\,ms$. A reasonably sized linac of $100 \div 300\,MeV$ would provide collision at J/ψ region with luminosity up to $\mathcal{L} \approx 10^{32}$.

A number of improvement which are planned for SPS in view of injection in LHC [16] with respect to the hardware for injection in LEP. They are taken into account, although their operability for electron beam, at much lower energy than proton beam, has to be asserted in further studies. The most relevant is the increase of the circulating bunches from 8 to 283 and the corresponding increase of current. A feedback system is planned to counteract the multibunch instability. Here it is assumed that it will work effectively for the positron too, although the shorter electron bunch with respect to the proton bunch is likely to excite a larger set of resonance in the SPS vacuum chamber.

The highest bunch charge accelerated for LEP injection is $10^{10}\,e^-/bunch$; machine study to increase LEP performances [17] indicated that up to $2.5 \cdot 10^{10}\,e^-/bunch$ could be possible; of course that study did not take into accont the improvements for the LHC injection system. This is the most critical point of this estimate. A deeper insight of the SPS performance with large positron circulating current must be the first point of any further study of this collider.

In the estimate of table 3 the nominal proton/bunch population $n_p = 10^{11}$ has been assumed for positron bunch too, since luminosity estimate can be easily derated to account for less populated bunches.

4 A linac-ring collider at PEP II

The current limit for the ring (PETRA, SPS) or the linac (CESR) forced the previous schemes to enhance the luminosity concentrating the available current in as few as possible bunches. This choice has a few drawbacks:

- the beam-beam perturbation is maximized
- the storable current is limited by the single bunch current limit, even if the multibunch instability is effectively counteracted.
- the high electron bunch charge n_e must be traded off with low ϵ_n.

These problems, but the last one, were to be faced also in the last generation of high luminosity storage rings (PEP II, KEK-B, DAΦNE); in all cases the choice was to trade off the problems of high current in few bunches with the complexity of a multibunch feedback system.

The same approach is followed in this section estimating the luminosity in collision between a 1658-bunch positron beam stored in the Low Energy Ring of PEP II (thereafter called LER) and an electron beam provided by a suitable CW superconducting linac.

The design luminosity of PEP II is $\mathcal{L} = 3 \cdot 10^{33}\, cm^{-2} s^{-1}$ with an electron currents of $0.98\ A$ in the HER [18]. Therefore the goal luminosity for the proposed collider can be obtained with a linac providing an average current of $\approx 1\, mA$.

A challenging program to realize high average current $< I >= 5\, mA$ in a superconducting linac with energy recovery has been recently successfully completed at the Jefferson Lab (a more detailed discussion is given in 5.1) , therefore a linac average current $< I >= 5\, mA$ has been assumed in the luminosity estimate.

The LER operates at $3.1\, GeV$ with a positron current of $2.14\ A$ distributed in 1658 bunches. The corresponding linac energy near the baryon pair threshold $\sqrt{s} \approx 1.9\, GeV$ is $\approx 300\, MeV$. This energy configuration provides less c.m. boosting ($\beta = 0.83$) in the laboratory frame with respect to previous schemes. As a rule of thumb, this increases the angular acceptance just above baryon pair threshold, but the detection efficiency reduction due to less energetic particles must be taken into account.

4.1 PEP II Low Energy Ring in parasitic mode

Two different beam size configurations at the interaction point have been considered, assuming that both have negligible dispersion there. The former assumes the value of the design optics of the $B - factory$. The latter has $\beta_x^\star$ and $\beta_z^\star$ exchanged. A radial vertical coupling $k = 0.04$ has been assumed in both cases since this is the conservative design value of the LER. Any improvement will positively affect both the luminosity and the linear tune shift.

Since the case $\beta_x^\star/\beta_z^\star << 1$ is the worst as far as the beam-beam perturbation is concerned, but provides the same luminosity and easier beam matching, it is taken here as a limit case. An intermediate lattice taking into account possible coupling improvements will provide the best trade off.

It is worth noting that in both cases the tune shift perturbation suffered by the stored positron beam is negligible, so parasitic operation should not affect the standard machine performances and setting, but for the lattice adjustments required by a second interaction region in the LER.

The luminosity estimates are reported in table 3. These configurations, which have the same emittance of the standard lattice give $\mathcal{L} = 1.6 \cdot 10^{31}\, cm^{-2}s^{-1}$;

The LER nominal horizontal emittance is $\epsilon_x = 6.4 \cdot 10^{-8}\, m \,@\, 3.1\, GeV$. Assuming that the same is required for the linac beam at $\approx 300\, MeV$, the gun must provide a beam with normalized emittance $\epsilon_- \approx 4 \cdot 10^{-5}\, m$. This parameter is in no way demanding for a sc linac beam.

4.2 PEP II Low Energy Ring in dedicated mode

The minimal horizontal emittance of a FODO lattice, as the PEP II rings, is given by

$$\epsilon_x^{min} = 4.52 \cdot 10^{-4} \frac{E^2}{J_x N_B^3}$$

where ϵ is in $meter \cdot radian$, E in GeV, N_B is the number of equal bending magnets along the orbit and J_X is the damping partition number. According to eq. 4.2 the minimal emittance of the Low Energy Ring, which is composed of 190 bending magnets, is $0.7 \cdot 10^{-9}\, m$ at $3.1\, GeV$. The large increase of emittance in the design lattice is the intentional effect of the wigglers in order to match the parameters of the High Energy Ring.

The emittance reduction gives a proportional increase of the luminosity. However it needs ≈ 100 times lower emittance of electron beam, i.e. $\epsilon_n^L \approx 0.4 \cdot 10^{-6}\, m$; this is challenging even at bunch charge $\ll 1$ nanoCoulomb. LER operation at $4\, GeV$ slightly relaxes the required linac emittance to $\epsilon_n^L \approx 0.8 \cdot 10^{-6}\, m$.

Operating LER in dedicated mode it is possible to exploit also a lower bunch frequency, increasing the e^+ bunch population up to the single bunch current limit, because most of the linac listed in section 5 have a larger bunch separation than LER.

This configuration, exploiting a low emittance lattice, can be intended for a second generation high statistics experiment at $\mathcal{L} > 10^{32}\, cm^{-2}s^{-1}$ compatible with synchrotron radiation experiments. It is worthwhile noting that collision of a $80\, MeV$ electron beam with the LER beam in this enhanced configuration would provide a $\Phi - factory$ with a luminosity $\mathcal{L} \geq 10^{33}\, cm^{-2}s^{-1}$ and a large boosting ($\beta_{CM} = 0.95$) in the laboratory frame.

4.3 PEP II at $\approx 2\,GeV$ c.m.

A more traditional approach lowering the PEP II c.m. energy down to $\approx 2\,GeV$ is to be taken into account too, at least for a cost/benefit comparison. This corresponds to operation of LER at $\approx 600\,MeV$ and HER at $\approx 1800\,MeV$ if energy is proportionally reduced in both rings. A further reduction of boosting ($\beta_{CM} = 0.53$)and a number of machine problems are to be taken into account.

A very preliminary estimate of the PEP II luminosity at $\approx 2\,GeV$ c.m. can be obtained with some scaling rules used in symmetric machines. It is alway assumed that luminosity is beam-beam interaction limited.

Assuming the natural scaling of emittance $\epsilon_x \propto E^2$ at fixed optics it is $\mathcal{L} \propto E^4$. This simple scaling must be taken with some care because the LER emittance is strongly depending on wiggler effect. The energy must be scaled by a factor 5 in each machine. Starting from a design luminosity of $3 \cdot 10^{33}@10\,GeV$ it is $\mathcal{L} = 4.8 \cdot 10^{30}@2\,GeV$. This result must be taken with a lot of care: operation of a storage ring at $E \approx E_{max}/5$ is probably troublesome since all the current instability threshold are lowered by a factor 5, and a number of effects, negligible at higher energy, can take place: e.g. the integrated luminosity is probably worsened by lifetime reduction due to the Touschek effect. A more detailed study of this option is underway [19], in view of the submission of a letter of intent to SLAC.

Moreover, in order to carry on any machine test a bypass is required to escape the BaBar detector which includes permanent magnets (quadrupole and bending) around the IP.

5 The superconducting linac

The linac beam quality parameters insofar assumed have been derived from those of the main present projects, namely the TESLA Test Facility at DESY and the FEL program at TJLAB. Since the technology of the superconducting accelerating structure is now well established and reliably operating in many laboratories, the most specific task in a small sc linac project is the construction of a low emittance injector providing a quasi CW beam with the required current and time structure. The injector parameters required for the linac ring collider are within the present or next-to-be state of art. Slightly different time structure of the bunch train is not likely to affect the beam quality, as far as a bunch charge $\geq 1\,nC$ is not required.

Thereafter the linac parameter list is tailored according to the performance required for a collider at PEP II, because it is the most powerful and lowest emittance linac. The crucial parameter for high luminosity in a linac-ring collider is indeed the average current and ultimately the electron beam power.

5.1 The energy recovery

A CW injector providing an electron beam at energy $E_e < 20\ MeV$ requires a reasonably costly rf power plant. The extention of the duty cycle δ of the full energy beam from $\delta \approx 0.01$ as in TTF up to $\delta = 1$ would require a huge rf plant. The beam dump and the related transfer line would pose by itself some problems due to the high energy deposition rate and intense neutron production. The energy recovery from the spent beam is therefore a mandatory achievement to reduce all the problems related to the large power carried by the beam.

In the energy recovery the used beam of energy E passes again in the linac at the opposite phase of the accelerating field and is decelerated down to the injection energy $E_{inj} \approx 10\ MeV$. Due to the very low rf losses in superconducting cavities this reduces the rf power requirement by nearly a factor E/E_{inj}, and mainly reduces the size and cost of the beam bump to a reasonable device which has to dissipate $< 100\,kW$; moreover, shielding are strongly simplified because electrons impinging the beam dump with energy $\leq 10\ MeV$ are below the neutron extraction threshold of most materials.

When this study began, the feasibility of a linac with energy recovery from the spent beam was not yet asserted, although this feature had been included in most sc linac development program [21]. In last months the full achievement of the design operational parameters of the IR Demo FEL at TJLAB set a milestone [20]. The experiment at TJLAB handled a spent beam which was degraded mainly by a large increase of energy spread, due to the FEL interaction, instead of an emittance increase, more peculiar to beam beam collision. The latter degradation is easier to manage so the the know-how from TJLAB will provide a sound basis for energy recovery after beam beam collision too, ensuring that a recirculated sc linac can be a part of a relible low energy e^+e^- collider.

Therefore, a linac providing a continuous train of bunches can be assumed since when the project of a linac ring collider will be defined the energy recovery technique, developped for large scale industrial plants based on high power FEL's, will have been consolidated and qualified for the most demanding applications.

5.2 The electron beam parameters

The normalized emittance ϵ_n which a linac gun must provide depends on the required emittance ϵ at the collision energy, according to the relation

$$\epsilon_n = \epsilon\gamma\beta \tag{19}$$

In order to get the best overlapping of the ring and linac beam it must be $\sigma_{x,z}^{Linac} = \sigma_{x,z}^{Ring}$. According to eq. 2÷3 this condition can be obtained with $\epsilon_p = \epsilon_n$ and $\beta_p = \beta_e$, or more generally with $\epsilon_p/\epsilon_n = \beta_e/\beta_p$; the former is certainly conservative, since the low energy electron beam can be shaped and squeezed more easily than the positron beam, but it is

assumed here for simplicity. The normalized emittance at the gun exit is then fixed for each configuration according to eq. 19.

The emittance of the ring and the normalized emittance of the linac for the configuration presented in sections 3 and 4 are summarized in table 3. Other gun and linac related parameters are listed in table 2. A brief summary of the operational or design performances of the main superconducting linacs in the world is given in section 5.3 for comparison.

5.3 A review of the sc linac

Superconducting linac in CW or high duty cycle mode are routinely operated, or in commissioning stage, in many laboratories. At Jefferson Lab CEBAF provides a beam at average current of $\approx 0.2\,mA$. . The TESLA Test Facility linac [27] at DESY has provided $8\,mA$ in long macropulses at 0.01 duty cycle. Two FEL facilities (SCA [23] at Stanford and ELBE [24] at FZR in Dresda) will exploit the TTF cavity, at reduced gradient, to provide a continuous beam of $1\,mA$.

The modified CEBAF module and the associated feedback system in the IR Demo FEL at TJLAB provided CW average current $< i >= 5\,mA$ at $48\,MeV$ with recovery of 75 % of the spent beam power back to the rf accelerating structures [29]; the residual $10\,MeV$ beam energy, corresponding to the injection energy, is required to handle the beam to the beam dump. The planned scaleup is toward a $10\,mA\ @\ 160\,MeV$ beam , which nicely fits, and also exceeds, the linac requirements for most of the collider considered in this note.

Therefore, a linac providing a beam current 10^3 times lower than the current of the HER appears feasible, according to the existing programs. This implies that the goal luminosity $\mathcal{L} \approx 10^{30} \div 10^{31}$ is readily achievable exploiting the state of art of sc linac design, without a dedicated R&D effort.

If higher performances are desired, comparable with the expected luminosity of the last generation of ring factories, the achievement of a high efficiency in energy recovery is mandatory because, e.g. in the dedicated PEP II -linac collider, the $5\,mA$ current provided by the linac would correspond to a beam power of $1.46\,MW$ to be wasted in the beam dump. Although the other configurations in section 3 require smaller linac, the beam power to waste is anyway in the hundreds of kW range.

Some of existing or planned superconducting linac, mainly operating as facility, and their parameters is reported in table 2.

Lab	**Sc linac**	**gun**	**energy** $[MeV]$	E_{acc} $[\frac{MeV}{m}]$	$I_{<macro>}$ $[mA]$	f_{bunch} $[MHz]$	**rf freq. sc cav.** $[GHz]$	**duty cycle** %	bunch charge pC	beam power $[kW]$	**emitt. norm.** $[\pi\mu m]$
Stanford	ps FEL center	THV	37	3	0.2	37	1.3	10	5.4	0.8	8
”	$\rightarrow$ upgraded [23]	THV		10			1.3	100			
Darmstadt	S-DALINAC	THV	38	5	0.06	10	3.0	100	6	2.3	..
TJLAB	CEBAF	THV	4000	14	0.16	1500	1.5	100	0.11	640	
TJLAB	IR Demo FEL [20]	PHV	42	14	5	37	15.5	100	135	210	12
TJLAB	IR-UV FEL [29]	PHV	200	14	5	25	1.5	100	200	1000	12
JAERI	IR-FEL [21]	THV	15	7	2	10	0.5	1	200	0.3	100
”	2-pass	THV	75	7	-	10	0.5	1			20
FZR	ELBE [24]	THV	20	10	1	12	1.3	100			1
DESY	TTF I [28]	THV	140	15	8	217	1.3	0.8	37	9	5
”	TTF II[28]	PRF	500	15	8	1	1.3	0.8	8000	32	20
”	TTF-UVFEL [27]	PRF	1000	25	8	9	1.3	0.8	890	64	1

Table 2: Overview of some superconducting electron linacs.

6 The luminosity

In the following table a summary of the performaces achievale using different combination of rings and linacs are reported. For each ring the table includes a line where the combinatin of minimal ring emittance and CW linac @ $< I >= 5\,mA$ is taken. These lines labelled *'ring name' +JLAB+*ϵ_{min} give a comparison of the beast conceivable performances.

A normalization to the same interaction point optics has been carried out as far as possible, using the values of the optical functions $\beta_x^* = 38\,cm,\ \beta_z^* = 1.5\,cm$ of the PEP II Low Energy Ring for the ring with beam energy up to $\approx 5\,GeV$ and $\beta_x^* = 50\,cm,\ \beta_z^* = 2.0\,cm$ of the High Energy Ring for the others. In some rows reporting the results of previous papers (row 1 and 4 for PETRA and CESR respectively) the original β^* values have been kept.

Conclusion

This review of the small number of rings suitable for a linac ring collider at $\sqrt{s} \approx 2\,GeV$ show that a luminosity in the range $\mathcal{L} > 10^{30}$ can be obtained in different configurations and sometimes largely exceeded.

Top performances require a linac gun emittance $\epsilon_n \approx 1\,\mu m$ and the most advanced beam handling technique. Machines capable of such high performances are in construction at major laboratories in the framework of TeV linear collider study or Free Electron research.

On the other hand the routinely operating range of the ring parameters ensures $\mathcal{L} \approx 10^{30}$. Running the ring at the minimal emittance, which is opposite to the HEP practice, but common in synchrotron radiation facility, improves the luminosity with a negligible beam beam perturbation.

The most intriguing point resulted the entangling between the detector and the machine components downstream the collision point. The effect on the geometrical acceptance is strongly depending on the angular opening of the nucleon pair. The efficiency is critically affected by both β_{CM} and the kinetic energy above the $n\bar{n}$threshold so the detector design and even the choice of E_p/E_e are depending on the interest of the experimental points just a few MeV above threshold.

#	Configuration	E_p/E_e $[GeV]$	$\epsilon^{ring}/\epsilon_n^{linac}$ $[\mu m]$	Coll. rate $[MHz]$	e^+/e^- $10^{11}/10^9$	β_x/β_z $[cm]$	Beam size $H \times V$ $[\mu m \times \mu m]$	ξ_x/ξ_z	Lumin. 10^{30} $[cm^{-2}s^{-1}]$
1	PETRA + TTF	7.0/0.14	0.022/6	$9 \cdot 0.01$	0.4/6.3	120/8	162×9.4	0.00/0.01	0.1
2	PETRA + JLAB + ϵ_{min}	7.0/0.14	0.002/0.5	37	0.1/0.8	50/2	33×1.5	0.01/0.01	48
3	CESR + TTF	5.3/0.19	0.340/125	$3 \cdot 0.01$	2.5/18	100/1.8	583×8	0.00/0.00	0.3
4	CESR + INJ + $\epsilon_{min} + J_x = 2$	5.3/0.19	0.024/9	5.4E-4	9/90	2.2/29	23×8	0.12/4.38	1.8
5	CESR + JLAB + ϵ_{min}	5.3/0.19	0.048/18	37	1.0/0.8	2.2/29	32×12	0.00/0.02	64
6	SPS + TTF	14/0.07	0.047/6.5	$11 \cdot 0.01$	1.0/4.7	50/2	153×7	0.00/0.00	0.4
7	idem + ϵ_{min}	14/0.07	0.009/1.2	$11 \cdot 0.01$	1.0/4.7	50/2	66×3	0.01/0.01	2.0
8	SPS + JLAB	14/0.07	0.047/6.5	11	1.0/2.9	50/2	153×7	0.00/0.00	24
9	idem + ϵ_{min}	14/0.07	0.009/1.2	11	1.0/2.9	30/2	66×6	0.01/0.01	130
10	PEP II + JLAB	3.1/0.29	0.064/40	249	0.14/0.6	38/1.5	153×6	≤ 0.001	16
11	PEP II + JLAB+ ϵ_{min}	3.1/0.29	0.001/0.8	249	0.14/0.6	38/1.5	21×1	0.01/0.01	1400
12	PEP II + JLAB+ ϵ_{min}	4.0/0.23	0.002/1.5	249	0.14/0.6	38/1.5	27×1	0.01/0.01	850

Table 3: Synoptic table of the luminosity estimates

The acronyms used in the configuration description have the following meanings:

- JLAB $\rightarrow < I >_{CW} = 5\,mA$ with energy recovery sc linac (see FEL program at Jefferson Lab)
- TTF $\rightarrow < I > macro = 8\,mA\,@\,9\,MHz \times 0.8\,ms \times 10\,Hz$ sc linac (see FEL program at DESY)
- INJ $\rightarrow < I >_{CW} = 20\,\mu A\,@\,4\,MHz \times 2.5\,\mu s \times 60\,Hz$, i.e. CESR injector
- $\epsilon_{min} \rightarrow$ minimal theoretical emittance achievable in that ring lattice $\epsilon[m] = 4.5 \cdot 10^{-4} N_{bend}^{-3} E^2[GeV]/J_x$

References

[1] C. Rubbia, 'A $\Phi \rightarrow K_L + K_S$ Factory using the Trieste Synchrotron Light Source' unpublished note, CERN 1988

[2] D.B.Cline and A.A.Garren, 'Study of Asymmetric ϕ Factory Options', Proceeding of EPAC 94, p. 461

[3] P. Grosse-Weismann, "Colliding a Linear Electron Beam with a Storage Ring Beam", Nucl. Instr. and Meth.A274,21(1989)

[4] P . Grosse-Weismann et al., 'Linac-Ring Collider B Factory', Proceeding of EPAC 90, p. 383

[5] A.Antonelli et al., Nucl. Phys. B 517(1998) 3

[6] Proceeding of the 'Nucleon structure workshop: FENICE experiment and investigation of the Neutron Form Factor', Frascati 1988

[7] A.Antonelli et al., Nucl. Instr. and Meth.A337 (1993) 34

[8] G.Bardin et al., Nucl. Phys. B 411(1994) 3

[9] P. Franzini, 'The muon giromagnetic ratio and R_H at DAΦNE', in The second DaΦNE physics handbook, vol. II p. 471

[10] M. Greco, 'On the Measurement of the hadronic Contribution to theMuon Anomalous Magnetic Moment', note LNF-88/24, submitted to 'Brevi Note' sect. of Il Nuovo Cimento A

[11] P.Patteri, 'The luminosity achievable in a linac-CESR collider based on the present performances and perspective', Wilson lab. note CBN 97-34

[12] FENICE Coll. and P.Patteri, πN newsletters 12 (1997) 73; R.Baldini et al., Nucl. Phys. 56B (1997) 275

[13] R. Baldini et al., 'A First Proposal for a New Measurement of the Nucleon Form Factors at an Asymmetric e^+e^-Collider', in 'Les Rencontres de Physique de la Vallèe d'Aoste - Results and perspectives in Particle Physics', Frascati Physics Series vol IX, Frascati 1997.

[14] R. Baldini et al.,Turkish Journal of Physics, 22 (1998) 645

[15] P.Patteri et al., Proceedings of the 1997 Particle Accelerator Conference, 572

[16] 'The SPS as Injector for LHC: Conceptual Design', CERN-SL/97-07 DI

[17] High luminosity option for LEP, CERN 91- 02/Erratum

[18] 'PEP-II, an asymmetric B factory: Conceptual Desgn Report. June 1993', SLAC-418

[19] M.Placidi, "The commissioning of PEP-II and its possible conversion into an Asymmetric Collider for measuring Nuleon Form Factors", Proc. NUCLEON'99 Workshop, Frascati, June 7-9, 1999

[20] G.R.Neil et al., 'First Operation of an FEL inj Same-cell Energy Recovery Mode', to appear in Proceedings of the 21^{th} International FEL Conference - Hamburg 1999

[21] Technical Digest of JAERI Satellite FEL meeting 1992

[22] H.Weise, 'The TESLA Test Facility (TTF) Linac - A Status Report', presented at the PAC'95;

[23] H.A.Schwettman, NIM A375 (1996) 632

[24] ELBE home page at www.fz-rossendorf.de

[25] T.I.Smith et al., NIM A296 (1990) 33

[26] M.Ohkubo et al., NIM A296 (1990) 270

[27] A VUV Free Electron Laser at the TESLA Test Facility at DESY - Conceptual Design Report, TESLA FEL 95-3, DESY 1995;

[28] TESLA Test Facility - Conceptual Design Report, TESLA Report 95-1, DESY 1995;

[29] S.Benson et al., 'Overview of the Jefferson Lab IR FEL Program' in Proceedings of the 18^{th} International FEL Conference - Rome 1996, Part II-28 , G.Dattoli and A.Renieri eds.